Research Article

URF PUBLISHERS
connect with research world

International Journal of Gastroenterology and Digestive Diseases

https://urfpublishers.com/journal/gastroenterology-digestive-diseases

Vol: 1 & Iss: 1

Mechanism of WYF in Treating Helicobacter Pylori Associated Gastritis Based on Network Pharmacology and Experimental Verification

Yuman Wang[1], Bingqian Fu[1], Xiao-yu Liu[1], Runze Li[1], Run-xue Sun[2], Wei-chao Xu[2], Shaopo-Wang[2], Yihao Xu[1] and Yan-ru Du[2]*

[1]Graduate School of Hebei University of Traditional Chinese Medicine, Hebei, 050011, China

[2]Hebei Hospital of Traditional Chinese Medicine, Hebei,050011, China

Citation: Wang Y, Fu B, Liu X-U, et al. Mechanism of WYF in Treating Helicobacter Pylori Associated Gastritis Based on Network Pharmacology and Experimental Verification. *J Gastro Dig Diseases*, 2026;1(1):01-06.

Received: 23 December, 2025; **Accepted:** 12 January, 2026; **Published:** 14 January, 2026

***Corresponding author:** Yan-ru Du, Hebei Hospital of Traditional Chinese Medicine, Hebei,050011, China

ABSTRACT

Objective: This study aims to systematically analyze the chemical components and core targets of Wenyang Huazhuo Qingjie Formula (WYF) through network pharmacology combined with in vitro experiments and to further explore the molecular mechanisms of WYF in treating Helicobacter pylori-associated gastritis (HpAG).

Method: Network pharmacology was employed to predict the potential chemical components, core targets and related signaling pathways of WYF in the intervention of HpAG. Subsequently, molecular docking technology was used to validate the interactions between the chemical components and core targets. An in vitro model of H. pylori-infected GES-1 cells was constructed and WYF was applied for intervention. Flow cytometry was used to detect the apoptosis rate of cells in each group, ELISA was performed to measure the levels of IL-8 and IL-10 in the cell supernatant and Western blot (WB) was utilized to assess the expression levels of JNK, NF-κB/p65 and p38MAPK proteins.

Result: Network pharmacology analysis revealed that quercetin, luteolin, β-sitosterol, kaempferol and apigenin in WYF are key chemical components for treating HpAG, with TP53, TNF, IL10, HIF1A and MAPK14 identified as the primary core targets. Molecular docking results demonstrated potential interactions between these chemical components and core targets. KEGG pathway analysis further indicated that WYF exerts its therapeutic effects mainly by regulating inflammation-related signaling pathways, such as the MAPK, NF-κB and p53 pathways. In vitro experimental results showed that WYF significantly reduced the apoptosis rate of H. pylori-infected GES-1 cells and enhanced cell viability. Additionally, WYF intervention markedly suppressed the expression of JNK and p38MAPK proteins while reducing the levels of IL-8 and IL-10.

Conclusion: WYF exerts therapeutic effects on HpAG through multiple targets and pathways, potentially involving the inhibition of the JNK/p38MAPK/IL-8/IL-10 signaling axis, thereby alleviating the inflammatory response in H. pylori-infected GES-1 cells. This study provides new molecular mechanistic insights into the treatment of HpAG with WYF and lays a theoretical foundation for its clinical application.

Keywords: Apoptosis, Helicobacter pylori-associated gastritis (HpAG), Wenyang Huazhuo Qingjie Formula (WYF), Network pharmacology, Molecular docking, Inflammation, JNK/p38MAPK signaling pathway

1. Introduction

Helicobacter pylori (Hp) is the most common and primary initiating factor of chronic gastritis[1]. According to statistics, the global infection rate of Hp was approximately 43.1% between 2011 and 2022, while the infection rate in China reached as high as 44.2%[2]. Hp infection is closely associated with the development of chronic gastritis, peptic ulcers and gastric cancer[3]. The pathogenesis of Hp-associated gastritis (HpAG) is complex and involves multiple factors, including Hp's motility apparatus, adhesin-mediated colonization and the invasion of host tissues by its virulence factors. Additionally, autoimmune responses, oxidative stress and inflammatory reactions play significant roles in the development and progression of HpAG[4]. Among these, inflammation and apoptosis are critical factors in the progression of HpAG.

Currently, there is no specific drug for the treatment of HpAG in Western medicine and the primary approach is symptomatic treatment, with the conventional regimen being antibiotic quadruple therapy. However, due to the overuse of antibiotics, the resistance of Hp to antibiotics has gradually increased and long-term high-dose use of antibiotics may lead to various adverse reactions, resulting in a year-by-year decline in the eradication rate of Hp[5]. In contrast, traditional Chinese medicine (TCM) has demonstrated unique advantages in eradicating Hp and alleviating the symptoms of HpAG[6,7]. TCM combines disease differentiation with syndrome differentiation to formulate herbal prescriptions, which can be used alone or in combination with antibiotics, thereby reducing the side effects of antibiotics, improving the eradication rate of Hp and enhancing the quality of life for patients.

Based on years of clinical experience in treating spleen and stomach diseases, Professor Li Diangui, a master of traditional Chinese medicine, proposed the "Turbid Toxin Theory." He believes that the key pathogenic factor of Hp-associated gastritis is the internal accumulation of turbid toxin. The basic pathogenesis involves external pathogens attacking and damaging the middle energizer (spleen and stomach), leading to spleen deficiency, dampness accumulation and turbid toxin formation. Over time, this transforms into heat and toxin accumulation, obstructing the movement of qi and causing yang qi stagnation and impaired warming function, ultimately resulting in the failure of the stomach to receive nourishment[8]. In clinical practice, Professor Li often employs the warming and clearing method and his classic formula, Wenyang Huazhuo Qingjie Formula (WYF), has shown significant efficacy in treating Hp-associated gastritis[9,10]. WYF is a classic TCM formula that has been used in clinical practice for nearly a decade. Its core concept is to warm spleen yang and resolve turbid toxin. The formula consists of the following herbs: Evodia rutaecarpa (3g), Zanthoxylum bungeanum (9g), Solanum nigrum (9g), Duchesnea indica (12g)， Agastache rugosa (12g)，Eupatorium fortunei (12g), Amomum villosum (12g)，Artemisia capillaris (20g)，Citrus aurantium (12g)，Magnolia officinalis (12g).

Although WYF has demonstrated clear therapeutic efficacy in the clinical treatment of HpAG, its specific mechanisms of action have not yet been fully elucidated. In this study, by integrating network pharmacology, molecular docking technology and in vitro experiments, we have revealed the molecular mechanisms through which WYF treats HpAG, primarily involving anti-inflammatory and anti-apoptotic effects. Furthermore, the study predicted five potential therapeutic targets, laying a theoretical and experimental foundation for further exploration of WYF's mechanisms of action in the future.

2. Materials and methods

2.1. Network pharmacology analysis

The active chemical components and core targets of Wenyang Huazhuo Qingjie Formula (WYF) were screened using the TCMSP database (http://tcmspw.com/tcmsp.php)11 and the TCMID database (http://119.3.41.228:8000/tcmid/). The screening criteria were set as oral bioavailability (OB) ≥ 30% and drug-likeness (D≥0.18. The Swiss Target Prediction database(http://www.swisstargetprediction.ch/) was further utilized to identify potential targets of the active components. HpAG-related target genes were obtained from the GeneCards and Disgenet databases. The intersection of drug targets and disease targets was identified and a Venn diagram was constructed to clarify the potential therapeutic targets of WYF for HpAG. Subsequently, the drug-component-target-pathway network was constructed using Cytoscape 3.9.0 software. The overlapping targets were imported into the STRING platform (https://string-db.org/) for protein-protein interaction (PPI) analysis and visualized using Cytoscape 3.9.0. Finally, Gene Ontology (GO) and Kyoto Encyclopedia of Genes and Genomes (KEGG) pathway enrichment analyses were performed using the Metascape database.

2.2. Molecular docking

The chemical components and core targets of WYF were selected for molecular docking validation. The structural files of the active chemical components and core targets were downloaded from the PubChem and PDB databases and saved in MOL and PDB formats, respectively. Crystal structures with high resolution, multiple ligands and complete structures were selected. The target protein receptors and ligand molecules were processed using AutoDock tools and molecular docking was performed using Autodock Vina to obtain binding energy data. Finally, the top binding compounds were visualized using PyMOL software.

2.3. Cell line and strain preparation

Human gastric mucosal epithelial cells (GES-1) and the Hp international standard strain NCTC11637: ATCC standard strain (43504) were purchased from Shanghai Enzyme Engineering Biotechnology Co., Ltd. The cells were co-cultured in a ratio of 100:1 for 12 hours to establish the Hp-infected cell model. After HE staining and observation under an electron microscope, GES-1 cells appeared predominantly triangular or spindle-shaped, arranged in a single layer, with a few suspended cells; cells were shed when growth became overly dense. Following the addition of Helicobacter pylori suspension and co-culturing for 12 hours, the cells became swollen and round, with vacuolization observed in the cytoplasm and an increase in suspended cells. The electron microscopy observations and a positive rapid urease test confirmed Hp infection in GES-1.

2.4. Preparation and grouping of experimental drugs Traditional Chinese Medicine (TCM)

WYF, composed of Evodia rutaecarpa (3g), Zanthoxylum bungeanum (9g), Solanum nigrum (9g), Duchesnea

ndica (12g), Agastache rugosa (12g), Eupatorium fortunei (12g), Amomum villosum (12g), Artemisia capillaris (20g), Citrus aurantium (12g) and Magnolia officinalis (12g), was prepared as instant granules (Guangdong Yifang Pharmaceutical Co., Ltd.). A total of 5.885 g of granules was dissolved in 100 mL of sterile water by ultrasonication at 60°C, resulting in a storage concentration of 58.85 mg/mL.

Western Medicine: The following drugs were used: Esomeprazole Magnesium Enteric-Coated Tablets (AstraZeneca, National Medicine Approval No. H20046379, 20 mg), Ornidazole Dispersible Tablets (Hunan Jiudian Pharmaceutical Co., Ltd., National Medicine Approval No. H20040460, 0.25 g), Amoxicillin Dispersible Tablets (Shanxi Tongda Pharmaceutical Co., Ltd., National Medicine Approval No. H20000492, 500 mg) and Bismuth Potassium Citrate Granules (Livzon Pharmaceutical Group, National Medicine Approval No. H10900086, 1.0 g). The four drugs were mixed and dissolved in 100 mL of sterile water by ultrasonication at 60°C, resulting in a storage concentration of 10 mg/mL.

Grouping: The experiment was divided into six groups，Blank group: Untreated GES-1 cells. Model group: Hp-infected GES-1 cells. Western medicine group: Hp-infected GES-1 cells treated with 5 μg/mL quadruple therapy. Low-concentration WYF group: Hp-infected GES-1 cells treated with 10 μg/mL WYF. Medium-concentration WYF group: Hp-infected GES-1 cells treated with 20 μg/mL WYF. High-concentration WYF group: Hp-infected GES-1 cells treated with 40 μg/mL WYF.

2.5. Determination of the maximum Non-Toxic Concentration of WYF on GES-1 Cells Using CCK-8 Assay

Cells from each group were seeded into 96-well plates and treated according to the grouping conditions. Except for the blank group, all other groups were co-cultured with Hp at a ratio of 100:1 (Hp to cells) for 12 hours. The model group was only infected with Hp, while the Western medicine group was treated with 5 μg/mL quadruple therapy. The low-, medium- and high-concentration WYF groups were treated with 10 μg/mL, 20 μg/mL and 40 μg/mL WYF, respectively. After 24 hours of incubation, CCK-8 solution was added and the absorbance (OD value) was measured to calculate cell viability. The cell viability was calculated using the formula: [(OD value of the experimental group - OD value of the blank group) / (OD value of the control group - OD value of the blank group)] × 100%.

2.6. Detection of apoptosis rate by flow cytometry

Hp-infected GES-1 cells were seeded into 6-well plates and treated according to the grouping conditions for 24 hours. Cells were collected, incubated at room temperature in the dark and resuspended in 500 μL of PBS buffer. The apoptosis rate was then measured using a flow cytometer.

2.7. Measurement of IL-8, IL-10 and IL-33 levels in cell supernatants by ELISA

Cell supernatants were collected and the levels of IL-8, IL-10 and IL-33 were measured according to the kit instructions. Ten standard wells were set up and the standards were serially diluted and added to the sample wells. After incubation at 37°C for 30 minutes, the plates were washed five times and 50 μL each of chromogenic reagent's A and B were added. The plates were then incubated at 37°C in the dark for 15 minutes, followed by the addition of stop solution for 15 minutes. The OD values were measured at 450 nm using a microplate reader and the concentrations of the inflammatory factors were calculated based on the standard curve.

2.8. Detection of JNK, p38MAPK and NF-κB/p65 protein expression by western blot

Cells from each group were collected and total protein was extracted using RIPA lysis buffer. Protein concentration was determined and the samples were denatured. SDS-PAGE gels were prepared and the proteins were separated by electrophoresis and then transferred to PVDF membranes. After blocking at room temperature for 2 hours, the membranes were incubated with primary antibodies, washed and then incubated with secondary antibodies. After another wash, the membranes were developed using chemiluminescence and the bands were scanned and analyzed using Tanon Gis software.

2.9. Statistical analysis

All experiments were repeated three times and the data were expressed as mean ± standard deviation (x ± s). Comparisons between two groups were performed using the two-sample t-test, while comparisons among multiple groups were performed using one-way ANOVA. A P-value < 0.05 was considered statistically significant. Data analysis was performed using SPSS 27.0 software.

3. Results

3.1. Network pharmacology

3.1.1. Active ingredients and target proteins of WYF and H.pAG: Through the TCMSP database, we identified a total of 100 active chemical components in Wenyang Huazhuo Qingjie Formula (WYF), including 2 from Magnolia officinalis, 8 from Agastache rugosa, 4 from Zanthoxylum bungeanum, 7 from Solanum nigrum, 7 from Eupatorium fortunei, 8 from Amomum villosum, 10 from Duchesnea indica, 24 from Evodia rutaecarpa, 13 from Artemisia capillaris and 17 from Citrus aurantium. After standardization and removal of duplicates using the UniProt database, 439 target proteins were obtained. Additionally, 281 targets related to Helicobacter pylori-associated gastritis (HpAG) were identified from the GeneCards and OMIM databases. The intersection of disease and drug targets yielded 67 common targets, which were considered potential key targets for WYF in treating HpAG **(Figure 1)**.

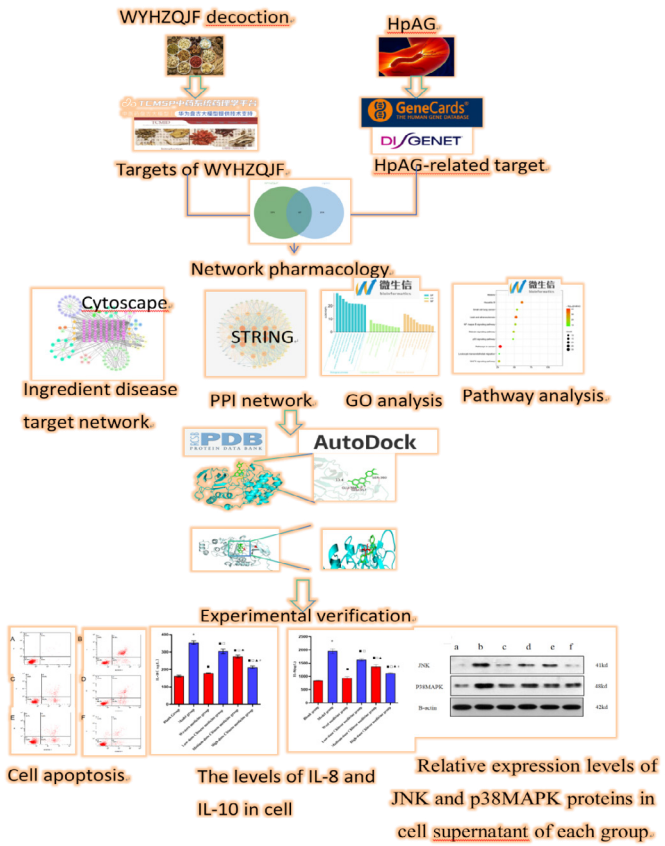

Figure 1: Workflow of the present study.

3.1.2. Herb-component-target network: The Venn diagram revealed 67 overlapping targets between WYF and HpAG **(Figure 2A)**, which were identified as the key targets for WYF in treating HpAG. Using Cytoscape 3.7.2 software, we constructed a herb-component-target network **(Figure 2B)**, which included 160 nodes and 449 edges. The interactions between these chemical components and core targets demonstrated the synergistic effects of multiple components and targets in WYF's therapeutic action against HpAG.

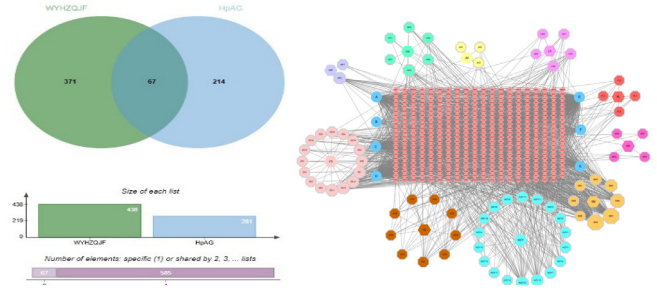

(A) (B)

Figure 2:(A) Venn diagram of WYF and HpAG target overlap. (B) Herb-compound-target network of WYF. Octagons represent the 10 herbs in WYF, circles represent compounds and diamonds represent potential targets.

Through network topology analysis, the top 10 active chemical components with the highest degree values were identified as quercetin, luteolin, beta-sitosterol, kaempferol, apigenin, isorhamnetin, nobiletin, beta-carotene, rutaecarpine and 7-hydroxycoumarin. These components were predicted to be the key active ingredients in WYF for intervening in HpAG **(Figure 3)**

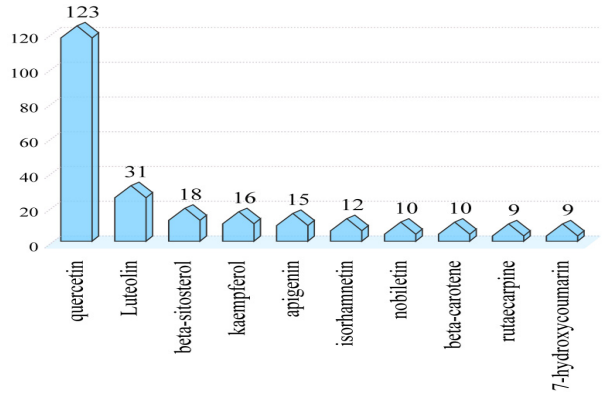

Figure 3: Top 10 active compounds in WYF based on degree values.

3.1.3. PPI network and core target prediction: The 67 overlapping targets were imported into the STRING platform to construct a protein-protein interaction (PPI) network **(Figure 4A)**. The top 15 core targets included TP53, NF, IL10, HIF1A, BCL2, AKT1, MMP9, EGFR, IL1B, NFKB1, EGF, PTGS2, MAPK14, MYC and TGFB1 **(Figure 4B)**. These targets are primarily associated with inflammation, apoptosis and oxidative stress. Additionally, other classical inflammatory targets, such as IL-8 and JNK, were validated in subsequent cellular experiments.

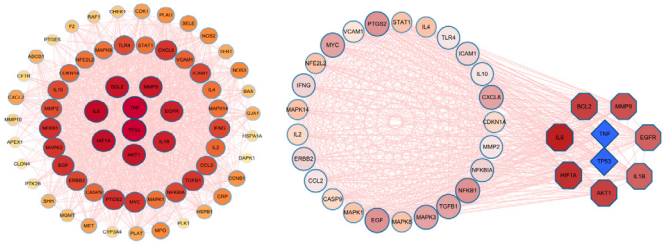

(A) (B)

Figure 4: (A) PPI network of shared targets between WYF and HpAG, (B) Core targets in the PPI network.

3.1.4. GO and KEGG enrichment analysis: To elucidate the potential mechanisms of WYF in treating HpAG, the 67 common targets were analyzed using the Metascape database for Gene Ontology (GO) and Kyoto Encyclopedia of Genes and Genomes (KEGG) enrichment analyses. The GO analysis results are shown in **(Figure 5A)**. For biological processes (BP), the targets were significantly enriched in positive regulation of cell migration, response to lipopolysaccharide, response to oxidative stress, cell population proliferation and cell activation. For cellular components (CC), the targets were primarily enriched in membrane rafts and vesicles. For molecular functions (MF), the targets were significantly enriched in signaling receptor activator activity, protein kinase activity, ubiquitin-like protein ligase binding, phosphatase binding and MAP kinase activity. The KEGG pathway enrichment analysis **(Figure 5B)** revealed that the targets were mainly associated with inflammation-related pathways, such as the MAPK signaling pathway, NF-kappa B signaling pathway and p53 signaling pathway.

3.1.5. Molecular docking results: The top five active chemical components of WYF-quercetin, luteolin, β-sitosterol, kaempferol and apigenin-were selected for molecular docking validation with five core targets: TP53 (3EXJ), TNF (2AZ5), IL10 (2H24), HIF1A (8HE0) and MAPK14 (6Y4X). A binding energy of ≤ −5.0 kcal/mol indicates that the ligand can bind to the receptor, while a binding energy of ≤ −7.0 kcal/mol suggests strong binding affinity.

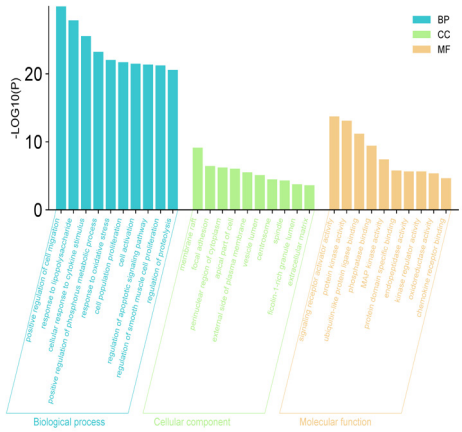

(A)

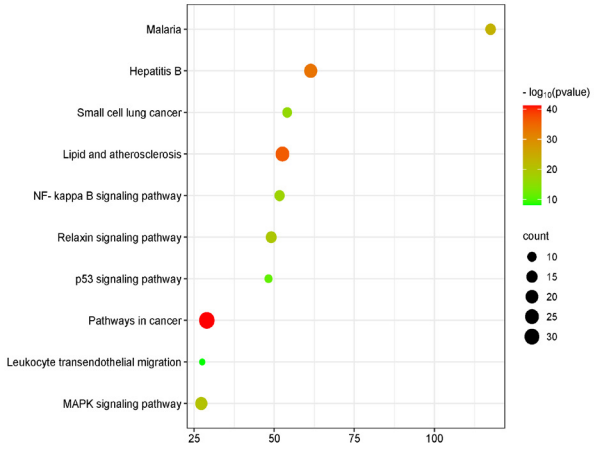

(B)

Figure 5A: GO function enrichment analysis of key targets of HpAG with WYF; B: KEGG pathway enrichment analysis of key targets of HpAG with WYF.

The results showed that, except for the pairs luteolin-8HE0, kaempferol-8HE0, kaempferol-3EXJ and apigenin-8HE0, all other core targets could bind to the active components. Notably, β-sitosterol exhibited binding energies of ≤ −7.0 kcal/mol with TP53, TNF, IL10, HIF1A and MAPK14, indicating strong binding affinity with these targets **(Table 1)**. The molecular docking results for the main components and core targets are illustrated in **(Figure 6)**.

3.2. Experimental validation

3.2.1. WYF inhibits the proliferation of GES-1 cells: The cell viability of GES-1 cells cultured at 37°C in a 5% CO_2 incubator for 24 hours was detected using the CCK-8 assay. The experimental results (Table 2) showed that when the concentration of WYF was 40 μg/mL, the cell viability of GES-1 cells was 98.5 ± 2.1%, with no significant statistical difference compared to the 0 μg/mL, 10 μg/mL and 20 μg/mL concentration groups ($P > 0.05$). However, when the concentration of WYF increased to 80 μg/mL, the cell viability of GES-1 cells significantly decreased to 88.2 ± 1.92%, showing a statistically significant difference compared to the 40 μg/mL concentration group ($P < 0.05$). These results indicate that WYF has no significant effect on the proliferation of GES-1 cells at concentrations below 40 μg/mL, but it significantly inhibits cell proliferation at concentrations above 80 μg/mL.

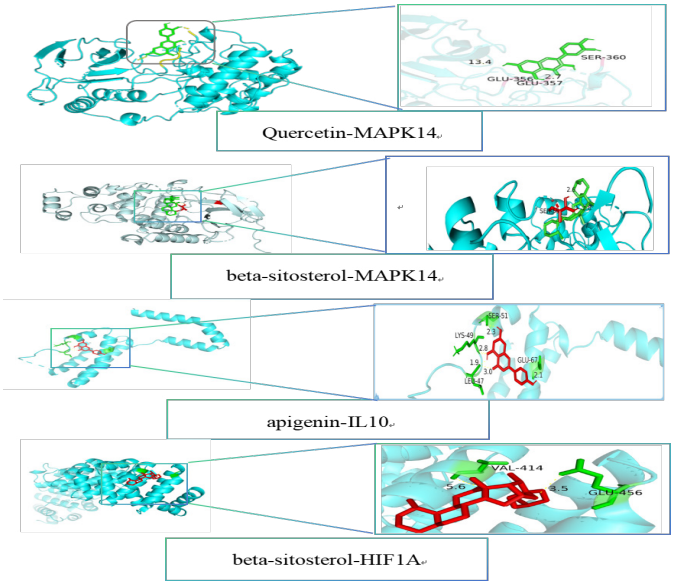

Figure 6: For combinations of major compounds and protein targets.

Table 1: Results of molecular docking.

Component-target	Binding energy
Quercetin-3EXJ	-5.26
Quercetin-6Y4X	-5.92
Quercetin-8HE0	-5.04
Quercetin-2H24	-4.29
Quercetin-2AZ5	-5.97
Luteolin-2AZ5	-6.72
Luteolin-2H24	-5.09
Luteolin-6Y4X	-5.82
Luteolin-8HE0	-4.87
Luteolin-3EXJ	-5.35
beta-sitosterol-2AZ5	-8.07
beta-sitosterol-2H24	-8.59
beta-sitosterol-6Y4X	-9.07
beta-sitosterol-8HE0	-8.44
beta-sitosterol-3EXJ	-7.46
Kaempferol-2AZ5	-5.97
Kaempferol-2H24	-5.02
Kaempferol-6Y4X	-6.75
Kaempferol-8HE0	-4.55
Kaempferol-3EXJ	-4.72
apigenin-3EXJ	-5.26
apigenin-8HE0	-4.75
apigenin-6Y4X	-6.87
apigenin-2AZ5	-6.65
apigenin-2H24	-5.48

Table 2: Effects of different concentrations on the viability of GES-1 cells.

drug level	The viability of the cells, (%)
0μg/mL	100
10μg/mL	98.52.1±
20μg/mL	98.62.25±
40μg/mL	95.12.01±*
80μg/mL	88.21.92±

3.2.2. WYF reduces Hp-induced apoptosis in GES-1 Cells: The apoptosis rate of Hp-induced GES-1 cells treated with Wenyang Huazhuo Qingjie Formula (WYF) was detected using Annexin V-FITC/PI double staining and flow cytometry **(Table 3, Figures 7 and 8)**. The results showed that compared to the blank group (1.566 ± 0.115%), the apoptosis rate in the model group (46.1 ± 0.624%) was significantly increased. In contrast, the apoptosis rates in the Western medicine group (25.666 ± 0.351%), low-concentration WYF group (32.266 ± 1.250%), medium-concentration WYF group (26.2 ± 0.953%) and high-concentration WYF group (14.533 ± 0.208%) were significantly reduced compared to the model group, with statistically significant differences ($P < 0.05$). Overall, these findings demonstrate that WYF can significantly reduce Hp-induced apoptosis in GES-1 cells.

Table 3: Apoptotic rates of cells in each experimental group.

Group	Apoptosis rate of the cells, (%)
blank group	1.5660.115±
model set	46.10.624±*
Western medicine group	25.6660.351±■
Low concentration of Chinese medicine group	32.2661.250±■□
Medium concentration of Chinese medicine group	26.20.953±■▲
High concentration of Chinese medicine group	14.5330.208±■□▲#

* P <0.05 compared with blank group, P <0.05 for ■ Western medicine group, low, medium and high concentrations, P <0.05 between ▲ mean and low concentration, P <0.05 for # mean and medium concentration.

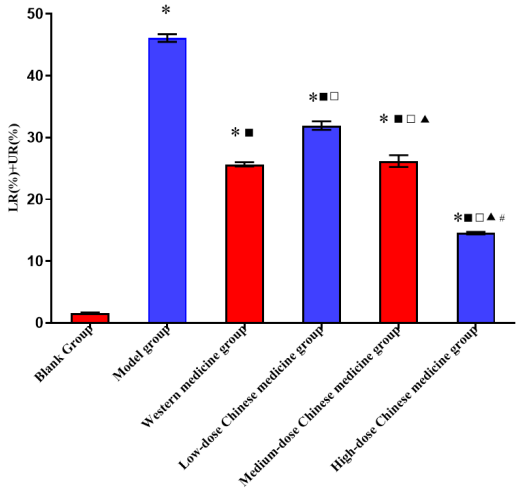

Figure 7: Cell apoptosis rate in each experimental group.

3.2.3. WYF suppresses Hp-induced inflammatory response in GES-1 cells

Inflammation is a key pathogenic mechanism in HpAG. The protein-protein interaction (PPI) network analysis indicated that NF, IL10 and MAPK14 are inflammation-related proteins involved in the regulation of HpAG by Wenyang Huazhuo Qingjie Formula. However, other classic inflammatory proteins, such as IL-8 and JNK, may also play significant roles. Therefore, to elucidate the mechanism of WYF in treating HpAG, we used ELISA to measure the levels of these inflammatory factors.

ELISA Detection of IL-8 and IL-10 Levels in Cell Supernatants **(Table 4, Figure 9)**

Compared to the blank group (843.649 ± 12.855 pg/mL), the level of IL-8 in the model group (1956.406 ± 89.192 pg/mL) was significantly increased ($P < 0.05$). In contrast, the levels of IL-8 in the Western medicine group (944.128 ± 50.935 pg/mL), low-concentration WYF group (1624.583 ± 49.129 pg/mL), medium-concentration WYF group (1365.919 ± 74.657 pg/mL) and high-concentration WYF group (1120.633 ± 22.487 pg/mL) were significantly reduced compared to the model group ($P < 0.05$).

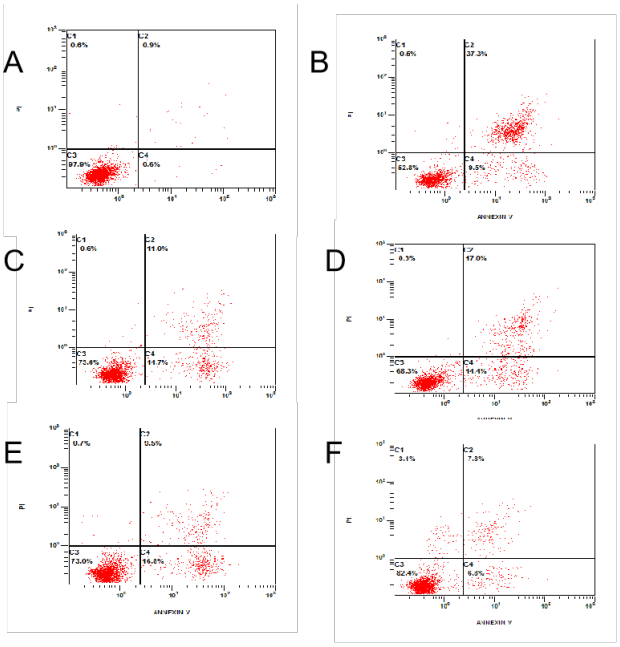

Figure 8: Cell apoptosis in each group Note A blank group B Model group C Western medicine Group D Low concentration group E medium concentration group F high concentration.

Compared to the blank group (162.102 ± 4.825 pg/mL), the level of IL-10 in the model group (354.104 ± 9.197 pg/mL) was significantly decreased ($P < 0.05$). Compared to the model group, the levels of IL-10 in the Western medicine group (178.99 ± 2.38 pg/mL), low-concentration WYF group (304.893 ± 13.344 pg/mL), medium-concentration WYF group (274.232 ± 7.783 pg/mL) and high-concentration WYF group (212.605 ± 7.332 pg/mL) were significantly reduced ($P < 0.05$), with statistical significance.

Table 4: Comparison of IL-8 and IL-10 levels in each group.

group	IL-8	IL-10
blank group	843.64912.855±	162.1024.825±
model set	1956.40689.192±*	354.1049.197±*
Western medicine group	944.12850.935±■	178.992.38±■
Low concentration of Chinese medicine group	1624.58349.129±■□	304.89313.344±■□
Medium concentration of Chinese medicine group	1365.91974.657±■□▲	274.2327.783±■□▲
High concentration of Chinese medicine group	1120.63322.487±■□▲#	212.6057.332±■□▲#

* The content of IL-8 and IL-10 increased with model group, P <0.05, P <0.05 with ■, P <0.05 with □ low, medium and high concentrations, P <0.05 with ▲ and low concentrations and P <0.05 with # mean vs. medium concentrations.

3.2.4. WYF inhibits the activation of the JNK/p38 MAPK signaling pathway: GO and KEGG enrichment analyses indicated that the MAPK signaling pathway might be involved in the inflammatory response process of G cells E by HelicobS-1

inducedacter pylori (Hp) under the intervention of WYF. Therefore, to determine the mechanism of action of WYF on HpAG, we employed Western blot to measure the relative expression levels of JNK and P38MAPK, which are proteins related to the MAPK signaling pathway **(Table 5 and Figure 10)**.

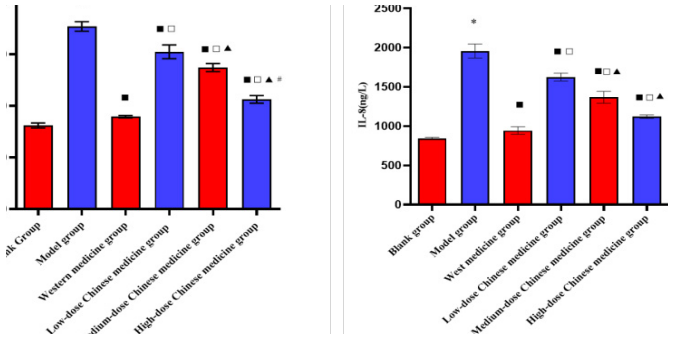

Figure 9: Level of IL-8 and IL-10 in the supernatants of cells from each.

Compared with the blank group (0.217 ± 0.061), the relative expression level of JNK protein in the model group (0.765 ± 0.06) was significantly increased ($P < 0.05$). When compared with the model group, the relative expression levels of JNK protein in the western - - group (medicine0.369 ± 0.016), the low - l WYF group (0ow-concentration.583 ± 0.095), the medium - concentration WYF group (0.456 ± 0.054) and the high - concentration WYF group (0.264 ± 0.04) were all significantly decreased ($P < 0.05$).

Similarly, compared with the blank group (0.279 ± 0.063), the relative expression level of p38MAPK protein in the model group (0.917 ± 0.126) was significantly increased ($P < 0.05$). When compared with the model group, the relative expression levels of p38MAPK protein in the western - - group (medicine0.472 ± 0.031), the low - l WYF group (0ow-concentration.618 ± 0.039), the medium - concentration WYF group (0.528 ± 0.058) and the high - concentration WYF group (0.349 ± 0.015) were all significantly decreased ($P < 0.05$).

In conclusion, WYF may alleviate the inflammatory response of G cells ES-1induced by Hp by regulating the MAPK signaling pathway, especially by inhibiting the expression of JNK and p38MAPK proteins.

Table 5: REL relative protein expression of JNK and p38MAPK in group 5.

group	JNK	P38 MAPK
blank group	0.2170.061±	0.2790.063±
model set	0.7650.06±*	0.9170.126±*
Western medicine group	0.3690.016±■	0.4720.031±■
Low concentration of Chinese medicine group	0.5830.095±■□	0.6180.039±■□
Medium concentration of Chinese medicine group	0.4560.054±■	0.5280.058±■
High concentration of Chinese medicine group		0.3490.015±■□▲

* $P < 0.05$ for comparison between model group and blank group, $P < 0.05$ for ■ Western medicine, low, medium and high concentrations, $P < 0.05$ for ▲ mean and low concentrations, $P < 0.05$ for # mean and medium concentration.

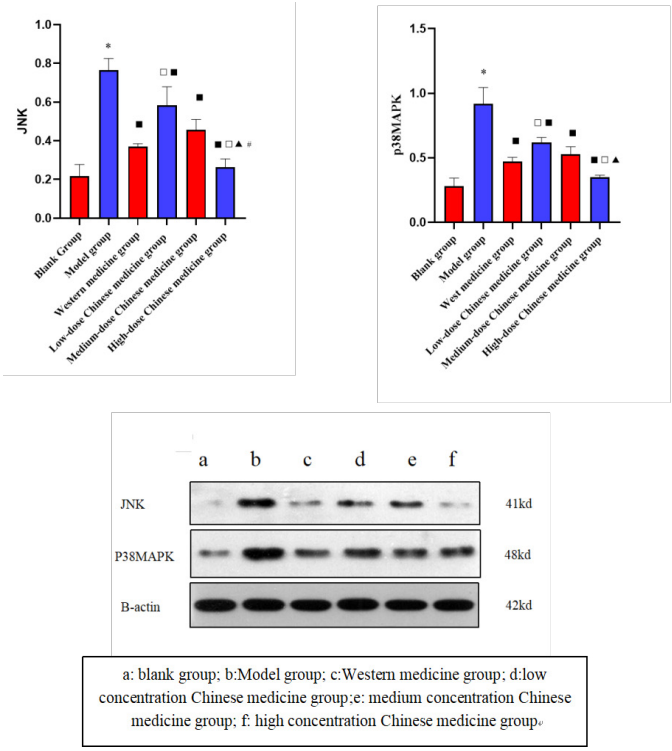

Figure 10: Relative expression levels of JNK and p38MAPK proteins in cell supernatant of each group

Discuss

Hp, a Gram-negative bacterium, is the primary pathogen responsible for 67%-80% of gastric ulcers and 95% of duodenal ulcers[12]. Globally, Hp infection is the most common cause of chronic gastritis and Hp-induced gastritis is considered a significant risk factor for peptic ulcers, their complications and gastric cancer[13-16]. Currently, the treatment of Hp-associated gastritis (HpAG) primarily relies on quadruple or triple therapy. However, due to the overuse of antibiotics, Hp resistance to antibiotics has gradually increased and the adverse effects of antibiotic treatment have become more frequent[17-19]. Therefore, finding effective treatments for HpAG with fewer adverse effects is of great importance. Traditional Chinese Medicine (TCM) has demonstrated unique advantages in the treatment of HpAG[20] and exploring therapeutic approaches from the perspective of TCM is worthy of in-depth research. The primary pathogenic mechanism of HpAG is closely related to inflammatory responses. The chronic inflammatory environment triggered by Hp infection activates multiple host intracellular signaling pathways, including inflammatory signaling pathways, further exacerbating gastrointestinal inflammation[21]. This suggests that inflammation is a key mechanism that requires focused attention in the treatment of HpAG.

In this study, we selected WYF, based on the "Turbid Toxin Theory," as the research subject to investigate its primary mechanisms in treating HpAG. WYF has shown significant efficacy in the clinical treatment of HpAG. Its formulation includes Evodia rutaecarpa (3g), Zanthoxylum bungeanum (9g), Solanum nigrum (9g), Duchesnea indica (12g), Agastache rugosa (12g), Eupatorium fortunei (12g), Amomum villosum (12g), Artemisia capillaris (20g), Citrus aurantium (12g) and Magnolia officinalis (12g). The formula collectively achieves the effects of warming yang, resolving turbidity and clearing toxins. Modern pharmacological studies have shown that the multiple components in WYF exhibit significant

pharmacological activities. For example, the volatile oils in Agastache rugosa have antibacterial and antiviral effects, while its polysaccharides demonstrate antitumor activity[22,23]. The active component evodiamine in Evodia rutaecarpa has anti-inflammatory and analgesic effects and its alkaloids exhibit broad-spectrum antitumor activity, with volatile oils inhibiting abnormal intestinal fermentation[24-26]. The oil from Zanthoxylum bungeanum alleviates cell activation and inflammatory responses by inhibiting the TLR2/MyD4/NF-κB signaling pathway[27]. Duchesnea indica has broad-spectrum antitumor effects and can be used in the treatment of various cancers, including gastric, intestinal and esophageal cancers[28,29]. Solanine in Solanum nigrum has anti-inflammatory and antihistamine effects and inhibits gastric and intestinal cancers[30,31]. The active components in Artemisia capillaris exhibit antibacterial and anti-inflammatory effects and can inhibit Hp urease activity[32,33].

In this study, we aimed to explore the potential mechanisms of WYF in improving HpAG, with a particular focus on its regulatory effects on inflammatory responses. Through network pharmacology analysis, we identified five major bioactive components in WYF-quercetin, luteolin, β-sitosterol, kaempferol and apigenin-that contribute to its therapeutic effects on HpAG. Previous studies have shown that these components have significant efficacy in alleviating HpAG. For example, quercetin reduces Hp-induced gastric epithelial cell apoptosis and inflammatory damage through the SP1/LCN1 axis and promotes macrophage M2 polarization[34]. Luteolin inhibits Hp growth and N-acetyltransferase activity while also exhibiting antitumor effects[35]. β-sitosterol demonstrates anti-inflammatory and anti-Hp activity[36]. Kaempferol exerts therapeutic effects through anti-inflammatory, antioxidant and anti-Hp adhesion mechanisms[37-39]. Apigenin reduces inflammation by decreasing Hp colonization levels, inhibiting NF-κB activation and reducing reactive oxygen species production. Our study suggests that WYF exerts anti-inflammatory effects through these five major bioactive components to treat HpAG, although the specific mechanisms require further investigation, potentially involving synergistic interactions among its multiple components.

Through protein-protein interaction (PPI) network analysis, we identified the top 15 core targets of WYF, including TP53, TNF, IL10, HIF1A, BCL2, AKT1, MMP9, EGFR, IL1B, NFKB1, EGF, PTGS2, MAPK14, MYC and TGFB1. These core targets are primarily associated with inflammation, apoptosis and oxidative stress. GO and KEGG enrichment analyses further indicated that the MAPK signaling pathway, NF-κB signaling pathway and p53 signaling pathway may be potential pathways through which WYF improves HpAG[40-44]. Molecular docking validation was performed using five core targets (TP53, TNF, IL10, HIF1A and MAPK14) and the five major chemical components. The results showed that these core targets could effectively bind to the main active components, suggesting that WYF may exert its effects through multiple components, targets and pathways.

To validate these findings, we conducted cell experiments focusing on the representative MAPK signaling pathway and related targets. c-Jun N-terminal kinase (JNK), a key member of the MAPK family, participates in cell proliferation, differentiation, apoptosis and inflammatory responses through phosphorylation. The p38MAPK signaling pathway can be activated by inflammatory factors (e.g., IL-8) and cytokines, playing a role in cell growth, differentiation, apoptosis and inflammatory responses. Studies have shown that Hp infection activates the JNK and p38MAPK signaling pathways[45] and pro-inflammatory factors such as IL-6 and IL-8 can further activate the p38MAPK signaling pathway, forming a positive feedback loop[46,47]. In our study, the apoptosis rate of GES-1 cells significantly increased after Hp infection, while WYF significantly reduced the apoptosis rate, maintaining cell stability. Additionally, after Hp infection, the levels of IL-8 and IL-10 were significantly elevated and the expression levels of JNK and p38MAPK proteins were also significantly increased, indicating that the pathogenesis of HpAG may be closely related to the JNK/p38MAPK signaling pathway. WYF may exert its therapeutic effects by blocking the JNK/p38MAPK signaling pathway, thereby alleviating inflammatory responses.

In summary, this study, through network pharmacology and in vitro cell experiments, demonstrated that WYF may treat HpAG by blocking the p38MAPK and JNK signaling pathways and reducing inflammatory responses. This provides important insights for TCM in the prevention and treatment of HpAG. However, this study has some limitations. First, we did not conduct a comprehensive pharmacological identification of WYF. Second, the research was limited to cell experiments and lacked animal experimental validation. Finally, the synergistic effects of the components in WYF and their specific mechanisms require further exploration. In future studies, we will further elucidate the synergistic effects of the components in WYF and explore other potential mechanisms of action in the treatment of HpAG.

5. Author Contribution

YM W: Conceptualization, Methodology, Writing - Original draft preparation, Revision and Editing, Experimental Verification.

BQ F: Conceptualization, Methodology, Experimental Verification, Data curation,

XY L,RZ L,RX S:Data collection, Preliminary analysis.

WC X,SP W,YH X: Literature review, Background research.

YR D: Supervision, Conceptual guidance, Writing - Reviewing and Editing. (†Corresponding author)

6. Data Availability Statement

Data is provided within the manuscript or supplementary information files.

7. Conflict of Interest

The authors declare that the research was conducted in the absence of any commercial or financial relationships that could be construed as a potential conflict of interest.

8. Ethical Approval

This paper does not deal with ethics.

Statement of Human and Animal Rights

This article does not address animal and human rights

Statement of Informed Consent

This paper does not involve human clinical studies, so there is no informed consent.

9. Acknowledgment statement

Thanks to all participants.

This work was partially funded by1. Science and Technology Project of the National Administration of Traditional Chinese Medicine, Project number: GDY-KJS-2023-013;

2.Hebei Province key research and development plan project, Chinese Medicine innovation special, project number :23377701D;

3. Project of Traditional Chinese Medicine Administration of Hebei Province, Project number: 2023019.

10. Fund Source

1. Science and Technology Project of the National Administration of Traditional Chinese Medicine, Project number: GDY-KJS-2023-013;

2.Hebei Province key research and development plan project, Chinese Medicine innovation special, project number :23377701D;

3. Project of Traditional Chinese Medicine Administration of Hebei Province, Project number: 2023019

11. Reference

1. Sedarat Z, Taylor-Robinson AW. Helicobacter pylori Outer Membrane Proteins and Virulence Factors: Potential Targets for Novel Therapies and Vaccines. Pathogens (Basel, Switzerland), 2024;13: 392.
2. Wei Y-F, Li X, Zhao M-R, Liu S, Min L, Zhu S-T, Zhang S-T, Xie S-A. Helicobacter pylori disrupt gastric mucosal homeostasis by stimulating macrophages to secrete CCL3. Cell Communication and Signaling: CCS, 2024;22(1):263.
3. Soares CDRR, Silva LMV, da Almeida BR, et al. Decreased Expression of Microrna-629 In Gastric Cancer Samples Potentiated by the Virulence Marker of h. Pylori, caga gene. Arquivos De Gastroenterologia, 2024;61: e23139.
4. Fan J, Zhu J, Xu H. Strategies of Helicobacter pylori in evading host innate and adaptive immunity: Insights and prospects for therapeutic targeting. Frontiers in Cellular and Infection Microbiology, 2024;14: 1342913.
5. Li X, Liu Y, Wang M, et al. Safety, pharmacokinetics and efficacy of rifasutenizol, a novel dual-targeted antibacterial agent in healthy participants and patients in China with Helicobacter pylori infection: Four randomized clinical trials. The Lancet. Infectious Diseases, 2024;24(6): 650-664.
6. Corrigendum: 2022 Chinese national clinical practice guideline on Helicobacter pylori eradication treatment. (2024). Chinese Med J, 2022;137: 1068.
7. Zhang H, Liu H. Mechanism of Weiwei granules in the treatment of chronic active Helicobacter pylori gastritis with atrophy based on the TLR4/NF-κB/COX-2 inflammatory signaling pathway. Histology and Histopathology, 2024;39: 761-769.
8. Guo Y, Jia X, Du P. Mechanistic insights into the ameliorative effects of Xianglianhuazhuo formula on chronic atrophic gastritis through ferroptosis mediated by YY1/miR-320a/TFRC signal pathway. J Ethnopharmacology, 2024;323: 117608.
9. Xia Z, Pingping C, Bin W. Discussion on the idea of Shengjiangsan for treating gastric cancer based on the theory of turbidity and toxicity. Chinese J Traditional Chin ese Med, 2024;39: 1840-1842.
10. Yuman W, Chongxin H, Xiaoyu L, Zhihua L, Yanru D. Effects of Wenyang Huazhuo Qingjie Fang on the expression of IceA and SabA genes and HSP70 and TRL4 in GES-1 cells infected with Hp. Lishizhen Traditional Chinese Medicine, 2023;34: 1088-1092.
11. Ru J, Li P, Wang J, et al. TCMSP: A database of systems pharmacology for drug discovery from herbal medicines. J Cheminformatics, 2014;6: 13.
12. Watari J, Chen N, Amenta PS, et al. Helicobacter pylori associated chronic gastritis, clinical syndromes, precancerous lesions and pathogenesis of gastric cancer development. World J Gastro, 2014;20: 5461-5473.
13. Li G-F, Qiao Y-W, Yu G. Helicobacter pylori Therapy and Risk of Gastric Cancer After Endoscopic Resection of Dysplasia: A Sensitivity Analysis Assessing Impact of Unmeasured Confounding. Gastroenterology, 2024;167: 417-418.
14. Xu H, Huang K, Shi M. MicroRNAs in Helicobacter pylori-infected gastric cancer: Function and clinical application. Pharmacological Res, 2024;205: 107216.
15. Yan T, Sun H, Liao Y, Zhou J. Helicobacter pylori mediated niche environment aberrations promote the progression of gastric cancer. Genes Diseases, 2024;11: 101207.
16. Zhou C, Bisseling TM, van der Post RS, Boleij A. The influence of Helicobacter pylori, proton pump inhibitor and obesity on the gastric microbiome in relation to gastric cancer development. Computational Structural Biotech J, 2024;23: 186-198.
17. Lee JH, Min B-H, Gong EJ, et al. Culture-based susceptibility-guided tailored versus empirical concomitant therapy as first-line Helicobacter pylori treatment: A randomized clinical trial. United European Gastro J, 2024.
18. Lim B, Kim KS, Ahn JY, Na K. Overcoming antibiotic resistance caused by genetic mutations of Helicobacter pylori with mucin adhesive polymer-based therapeutics. Biomaterials, 2024;308: 122541.
19. Sun C, Huang J, Guo X. An all-in-one therapeutic platform for the treatment of resistant Helicobacter pylori infection. Biomaterials, 2024;308: 122540.
20. Li Y, Li X, Tan Z. An overview of traditional Chinese medicine therapy for Helicobacter pylori-related gastritis. Helicobacter, 2021;26: 12799.
21. Zhou A, Li L, Zhao G, et al. Vitamin D3 Inhibits Helicobacter pylori Infection by Activating the VitD3/VDR-CAMP Pathway in Mice. Frontiers in Cellular and Infection Microbiology, 2020;10: 566730.
22. Feng B, Zhu Y, Su Z, Tang L, Sun C, Li C, Zheng G. Basil polysaccharide attenuates hepatocellular carcinoma metastasis in rat by suppressing H3K9me2 histone methylation under hepatic artery ligation-induced hypoxia. Int J Bio Macromolecules, 107(Pt B), 2018: 2171-2179.
23. Zhan Y, An X, Wang S, Sun M, Zhou H. Basil polysaccharides: A review on extraction, bioactivities and pharmacological applications. Bioorganic Med Chem, 2020;28: 115179.
24. Panda M, Tripathi SK, Zengin G, Biswal BK. Evodiamine as an anticancer agent: A comprehensive review on its therapeutic application, pharmacokinetic, toxicity and metabolism in various cancers. Cell Biology and Toxicology, 2023;39: 1-31.
25. Tan Q, Zhang J. Evodiamine and Its Role in Chronic Diseases. Adv in Experimental Med Bio, 2016;929: 315-328.
26. Yu Y, Huang X, Liang C, Zhang P. Evodiamine impairs HIF1A histone lactylation to inhibit Sema3A-mediated angiogenesis and PD-L1 by inducing ferroptosis in prostate cancer. European J Pharmacology, 2023;957: 176007.
27. Hou J, Wang J, Meng J, et al. Zanthoxylum bungeanum Seed Oil Attenuates LPS-Induced BEAS-2B Cell Activation and Inflammation by Inhibiting the TLR4/MyD88/NF-κB Signaling Pathway. Evidence-Based Complementary and Alternative Medicine: eCAM, 2021;2021: 2073296.

28. Liu X, Wang K, Wang L, Fan X. Network Pharmacology Combined with Experimental Validation Reveals the Anti-tumor Effect of Duchesnea indica against Hepatocellular Carcinoma. Journal of Cancer, 2023;14: 505-518.

29. Mohibullah, Pirzada AS, Aschner M, Khan H. Anxiolytic and antidepressant potential of extracts of Duchesnea Indica in animal models. PHYTOnutrients (Karachi, Pakistan), 2022;1: 48-56.

30. Keuter L, Wolbeck A, Kasimir M, Schürmann L, Behrens M, Humpf H-U. Structural Impact of Steroidal Glycoalkaloids: Barrier Integrity, Permeability, Metabolism and Uptake in Intestinal Cells. Molecular Nutri Food Res, 2024;68: 2300639.

31. Pei H, Yang J, Li W, et al. Solanum nigrum Linn.: Advances in anti-cancer activity and mechanism in digestive system tumors. Medical Oncology (Northwood, London, England), 2023;40: 311.

32. Nechita M-A, Pralea I-E, Țigu A-B, et al. Agastache Species (Lamiaceae) as a Valuable Source of Volatile Compounds: GC-MS Profiling and Investigation of In Vitro Antibacterial and Cytotoxic Activities. Int J Molecular Sci, 2024;25: 5366.

33. Song J-H, Nam H-H, Park I. Comparative Morphology of Island and Inland Agastache rugosa and Their Gastroprotective Effects in EtOH/HCl-Induced Gastric Mucosal Gastritis. Planta Medica, 2024;90: 4-12.

34. Wang Z, Zhou X, Hu X, Zheng C. Quercetin ameliorates Helicobacter pylori-induced gastric epithelial cell injury by regulating specificity protein 1/lipocalin 2 axes in gastritis. J Appl Toxicology: JAT, 2024;44: 641-650.

35. Chung JG, Hsia TC, Kuo HM, Li YC, Lee YM, Lin SS, Hung CF. Inhibitory actions of luteolin on the growth and arylamine N-acetyltransferase activity in strains of Helicobacter pylori from ulcer patients. Toxicology in Vitro: An International Journal Published in Association with BIBRA, 2001;15: 191-198.

36. Quílez A, Berenguer B, Gilardoni G, et al. Anti-secretory, anti-inflammatory and anti-Helicobacter pylori activities of several fractions isolated from Piper carpunya Ruiz Pav. J Ethnopharmacology, 2010;128: 583-589.

37. Kim KA, Kang D-M, Ko Y-J, et al. Chaenomelin, a New Phenolic Glycoside and Anti-Helicobacter pylori Phenolic Compounds from the Leaves of Salix chaenomeloides. Plants (Basel, Switzerland), 2024;13: 701.

38. Yang R, Li J, Wang J, Wang Y, Ma F, Zhai R, Li P. Kaempferol inhibits the growth of Helicobacter pylori in a manner distinct from antibiotics. J Food Biochem, 2022;46: 14210.

39. Yi R, Wang F-B, Tan F, Long X, Pan Y, Zhao X. Intervention effects of lotus leaf flavonoids on gastric mucosal lesions in mice infected with Helicobacter pylori. RSC Advances, 2020;10: 23510-23521.

40. Cheng W, Liao Y, Xie Y, et al. Helicobacter pylori-induced fibroblast-derived Serpin E1 promotes gastric cancer growth and peritoneal dissemination through p38 MAPK/VEGFA-mediated angiogenesis. Cancer Cell Int, 2023;23: 326.

41. Domínguez-Martínez DA, Fontes-Lemus JI, García-Regalado A, Juárez-Flores Á, Fuentes-Pananá EM. IL-8 Secreted by Gastric Epithelial Cells Infected with Helicobacter pylori CagA Positive Strains Is a Chemoattractant for Epstein-Barr Virus Infected B Lymphocytes. Viruses, 2023;15: 651.

42. Huang H, Wu D, Li Q, et al. Jiegeng decoction ameliorated acute pharyngitis through suppressing NF-κB and MAPK signaling pathways. J Ethnopharmacology, 2024;332: 118328.

43. Karayiannis I, Martinez-Gonzalez B, Kontizas E, et al. Induction of MMP-3 and MMP-9 expression during Helicobacter pylori infection via MAPK signaling pathways. Helicobacter, 2023;28: 12987.

44. Sharafutdinov I, Backert S, Tegtmeyer N. The Helicobacter pylori type IV secretion system upregulates epithelial cortactin expression by a CagA- and JNK-dependent pathway. Cellular Microbiology, 2021;23: 13376.

45. Tang W, Guan M, Li Z, Pan W, Wang Z. A2BR facilitates the pathogenesis of H. pylori-associated GU by inducing oxidative stress through p38 MAPK phosphorylation. Heliyon, 2023;9: 21004.

46. El-Shoura EAM, Abdelzaher LA, Ahmed AAN, et al. Reno-protective effect of nicorandil and pentoxifylline against potassium dichromate-induced acute renal injury via modulation p38MAPK/Nrf2/HO-1 and Notch1/TLR4/NF-κB signaling pathways. Journal of Trace Elements in Medicine and Biology: Organ of the Society for Minerals and Trace Elements (GMS), 2024;85: 127474.

47. Yu L, Qin J-Y, Sun C, et al. Xianglian Pill combined with 5-fluorouracil enhances antitumor activity and reduces gastrointestinal toxicity in gastric cancer by regulating the p38 MAPK/NF-κB signaling pathway. J Ethnopharmacology, 2024;326: 117988.